Molecular Sugar Sticks: Cylindrical Glycopolymer Brushes

Sharmila Muthukrishnan,[†] Mingfu Zhang,[†,‡] Markus Burkhardt,[†] Markus Drechsler,[†] Hideharu Mori,[§] and Axel H. E. Müller*[,†]

Makromolekulare Chemie II and Bayreuther Zentrum für Kolloide und Grenzflächen, Universität Bayreuth, D-95440 Bayreuth, Germany, and Department of Polymer Science and Engineering, Faculty of Engineering, Yamagata University, 4-3-16, Jonan, Yonezawa, 992-8510, Japan

Received July 11, 2005

ABSTRACT: We report the synthesis of glycocylindrical brushes ("molecular sugar sticks") with poly(3-*O*-methacryloyl-α,*β*-D-glucopyranose) (PMAGlc) side chains, using the "grafting from" approach via atom transfer radical polymerization (ATRP) of the protected monomer, 3-*O*-methacryloyl-1,2:5,6-di-*O*-isopropylidene-D-glucofuranose (MAIGlc). The formation of well-defined brushes with a narrow length distribution was confirmed by gel permeation chromatography with multiangle light scattering detector (GPC-MALS) and ^{1}H NMR. The initiating efficiency of the initiating sites of the polyinitiator poly(2-(2-bromoisobutyryloxy)ethyl methacrylate) were determined to be in the range $0.23 < f < 0.38$ by cleaving the side chains from the backbone. The cleaved side chains were analyzed using ^{1}H NMR, GPC/viscosity, and GPC-MALS measurements. Despite the rather low initiating efficiency, the glycocylindrical brushes show the characteristic wormlike structure, as visualized by scanning force microscopy (SFM). The deprotection of the isopropylidene groups of the poly(3-*O*-methacryloyl-1,2:5,6-di-*O*-isopropylidene-D-glucofuranose) (PMAIGlc) side chains resulted in water-soluble glycocylindrical brushes. SFM measurements, cryogenic transmission electron microscopy, and dynamic light scattering show a stretched, wormlike structure.

Introduction

Regular comblike polymers exhibit the structure of cylindrical brushes if the side chains are densely grafted; that is, every monomer unit of the main chain carries a side chain, and the main chain is longer than the side chains. In the past, three routes for preparing cylindrical brushes have been used, that is, the "grafting through", "grafting onto", and "grafting from" approaches. The first method, the conventional radical polymerization of macromonomers (grafting through),[1,2] typically results in a broad chain length distribution of the resulting polymer and incomplete macromonomer conversion. The grafting onto technique[3,4] allows the use of well-defined main chain and side chains but has often suffered from insufficient grafting efficiency. Finally, in the grafting from approach, side chains of the brush have been formed via atom transfer radical polymerization (ATRP) initiated by pendant initiating groups on the backbone.[5−7] This method resulted in well-defined polymer brushes with a high grafting density and narrow length distributions of the backbone. The purification of the resulting cylindrical brushes was much simpler compared to the other two methods.

Using ATRP in the grafting from approach, we have recently reported the synthesis of cylindrical polymer brushes with polystyrene (PS), poly(*n*-butyl acrylate) (P*n*BA), poly(*tert*-butyl acrylate) (P*t*BA), and poly(acrylic acid) (PAA) side chains as well as of core−shell brushes with amphiphilic block copolymer side chains, for example, PAA-*b*-PS or PAA-*b*-P*n*BA.[6,8] The ability of the hydrophilic PAA core of the amphiphilic core−shell brushes to coordinate with different metal cations was used for the synthesis of novel organic/inorganic hybrid nanocylinders.[9−11]

Here, we report on the synthesis and characterization of cylindrical polymer brushes comprised of poly(3-*O*-methacryloyl-1,2:5,6-di-*O*-isopropylidene-α-D-glucofuranoside) (PMAIGlc) side chains, using the grafting from approach via ATRP. After deprotection, the water-soluble cylindrical glycopolymer brush poly(3-*O*-methacryloyl-1,2:5,6-di-*O*-isopropylidene-α,*β*-D-glucofuranose) (PMAIGlc) was obtained.

Recently, considerable attention has been paid to the design of biofunctional materials carrying the ligand on synthetic polymers. Synthetic carbohydrate polymers with biocompatible and biodegradable properties can be used for investigating carbohydrate-based interactions.[12] Carbohydrate-based monomers and polymers confer a high hydrophilicity and water solubility and thus are of main interest with respect to very specialized applications in basic biochemical and biomedical research such as molecular recognition processes,[13] drug delivery systems,[14,15] and also surfactants.[16]

ATRP has been used for the synthesis of many sugar-carrying block,[17,18] graft,[19] and hyperbranched polymers.[20,21] In this paper, we have employed ATRP for the synthesis of glycocylindrical brushes using a bulky sugar-carrying methacrylate monomer, poly(3-*O*-methacryloyl-1,2:5,6-di-*O*-isopropylidene-α-D-glucofuranose) (PMAIGlc), via the grafting from approach. Cylindrical glycopolymer brushes are architecturally interesting, because of the possibility to form extended chain conformations, based on the intramolecular excluded-volume interactions between bulky side chains densely grafted to the backbone. The synthetic route leading to the glycopolymer brushes is outlined in Scheme 1.

Experimental Section

Materials. CuBr (95%, Aldrich) was purified by stirring overnight in acetic acid. After filtration, it was washed with

* To whom correspondence should be addressed. E-mail: axel.mueller@uni-bayreuth.de. Fax: +49 (921) 55-3393.
† Universität Bayreuth.
‡ Present address: Polymer Science and Engineering, University of Massachusetts, Amherst, MA 01003.
§ Yamagata University.

10.1021/ma0515073 CCC: $30.25
Published on Web 08/19/2005

Scheme 1. General Route to the Synthesis of Glycocylindrical Brushes

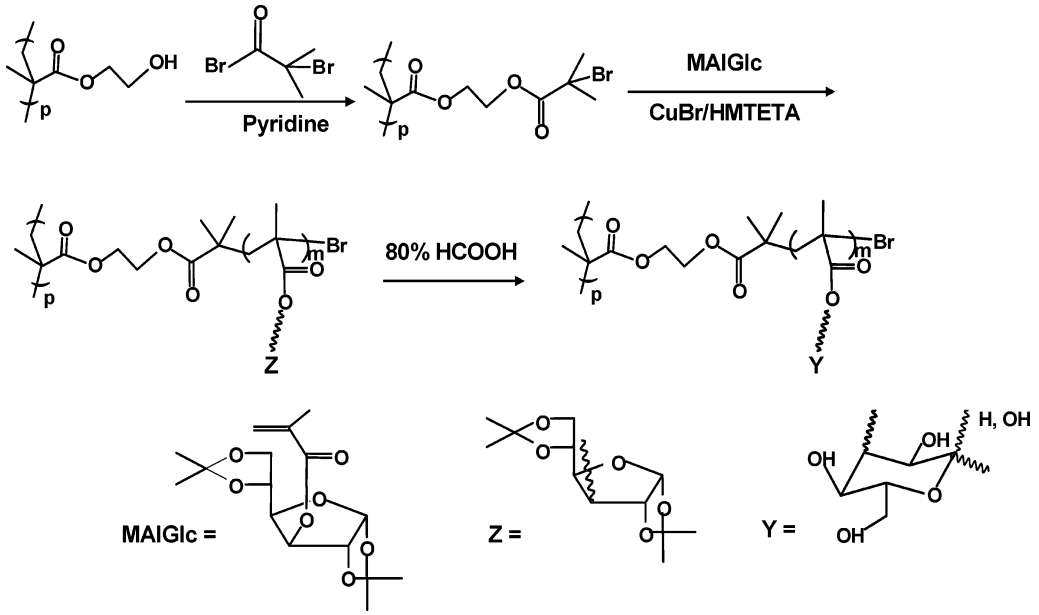

Table 1. Synthesis and Characterization of Short and Long Glycocylindrical Brushes via ATRP[a]

brush	initiator	$[M]_0/[I]_0$	time (min)	conv[b] (%)	$10^{-4}M_{n,GPC}$[c]	PDI[c]	$10^{-4}M_{n,MALS}$	$DP_{n,sc,calcd}$[d]	R_g (nm)
1	PBIEM-I	100	10	11.0	6.63	1.19	59	6.6	25.6 ± 0.4
2	PBIEM-I	300	20	9.3	8.91	1.18	150	19	27.1 ± 0.5
3	PBIEM-I	400	40	10.0	17.8	1.25	180	22	31.2 ± 0.4
4	PBIEM-II	300	30	5.0	40.8	1.19	900	18	41.5 ± 0.1
5	PBIEM-II	200	25	10.0	58.6	1.07	1120	22	59.5 ± 0.3

[a] Solution polymerization in ethyl acetate (50 wt % to MAIGlc) at 60 °C at constant $[I]_0/[CuBr]_0/[HMTETA]_0 = 1/0.5/0.5$. [b] Determined by ^{1}H NMR. [c] Determined by GPC using THF as eluent with PS standards. [d] Calculated from $M_{n,MALS}$, assuming a 100% initiation efficiency according to $DP_{sc,calcd} = (M_{n,brush} - M_{n,backbone})/(DP_{n,bb}M_0)$, where $DP_{n,bb}$ is the degree of polymerization of the backbone and M_0 is the molecular weight of HEMA.

ethanol and ether and then dried. 1,1,4,7,10,10-Hexamethyltriethylenetetramine (HMTETA, 97%, Aldrich) was distilled and degassed before use. Sodium methoxide (25% in methanol, Aldrich) was used as received. 3-*O*-Methacryloyl-1,2:5,6-di-*O*-isopropylidene-D-glucofuranose (MAIGlc) was synthesized by the reaction of 1,2:5,6-di-*O*-isopropylidene-D-glucofuranose and methacrylic anhydride in pyridine and purified by vaccum distillation as reported by us recently.[21] The synthesis and characterization of the two poly(2-(2-bromoisobutyryloxy)ethyl methacrylate) polyinitiators (PBIEM-I and PBIEM-II) employed for the synthesis of the polymer brushes were described in an earlier publication.[6,8] PBIEM-I was prepared by the reaction of bromoisobutyryl bromide with poly(2-hydroxyethyl methacrylate) (PHEMA) obtained by ATRP. PBIEM-II was synthesized from PHEMA obtained via anionic polymerization of trimethylsilyl-protected HEMA. ^{1}H NMR ($CDCl_3$): $\delta = 4.37$, 4.21 ($-CH_2-OCO-$), 2.20−1.40 ($-CH_2-C$), 1.97 [$-C(Br)-(CH_3)_2$], 1.30−0.70 ($-CH_3$) ppm.

Polymerizations. All polymerizations were carried out in a round-bottom flask sealed with a plastic cap. A representative example for the synthesis of a cylindrical brush is as follows: To a round-bottom flask containing CuBr (2.7 mg, 0.0190 mmol) and MAIGlc (2.5 g, 7.62 mmol) in ethyl acetate (2.5 g, 50 wt %) was added the polyinitiator PBIEM-II (10.6 mg, 0.0381 mmol of initiating α-bromoester group) (see Table 1), and this was stirred for 10 min to dissolve the polyinitiator completely. Then, HMTETA (4.3 mg, 0.0190 mmol) was added to this mixture and the color changed to green, indicating the start of polymerization. The flask was then placed in an oil bath at 60 °C for 25 min. Monomer conversion as detected by ^{1}H NMR was 10%. The contents of the flask, which were very viscous even at such a low conversion, were then dissolved in tetrahydrofuran (THF). The solution was passed through a silica column, and the polymer was precipitated from THF into methanol two times. Then, it was precipitated in petroleum ether twice to remove the unreacted monomer completely. Finally, the product was freeze-dried from dioxane and dried under vacuum at room temperature. The polymer had $M_n = 58.6 \times 10^4$ and $M_w/M_n = 1.07$ according to conventional GPC using PS calibration and $M_n = 1120 \times 10^4$ and $M_w/M_n = 1.09$ as determined by gel permeation chromatography with multiangle light scattering detector (GPC-MALS) measurement. The polymer was soluble in THF and chloroform but insoluble in methanol, acetone, and water.

Deprotection. The transformation of sugar sticks containing poly(MAIGlc) side chains into water-soluble polymer with poly(3-*O*-methacryloyl-α,β-D-glucopyranose) (PMAGlc) side chains was achieved under mildly acidic conditions.[21] The polymer (100 mg) was dissolved in 80% formic acid (12 mL) and stirred for 48 h at room temperature. Then, 5 mL of water was added and it was stirred for another 3 h. The solution was dialyzed using a Spectra/Por^R dialysis tube (MWCO: 1000) against Millipore water for 2 days. The resulting polymer was freeze-dried from water and dried under vacuum. The deprotected polymer was obtained as white powder which was soluble in water and methanol but insoluble in THF and acetone.

Solvolysis of the Glycocylindrical Brushes. The solvolysis of the brushes was achieved via base-catalyzed transesterification in methanol.[22] The polymer (20 mg) was dissolved in THF in a capped vial. Methanol was added until the polymer was precipitated, and then, sodium methoxide (25% in methanol, four to five drops) was added. The capped vial was then placed in an oil bath and kept at 90 °C for 7 days. Then, the solution was cooled and stirred for 2 h in the presence of cationic ion-exchange resin (Dowex MSC-1). The solution was decanted and evaporated. The molecular weight of the resulting product was analyzed using conventional GPC, GPC/viscosity, and GPC-MALS measurements.

Characterization. The apparent molecular weights of the brushes and cleaved side chains were characterized by conventional GPC using THF as eluent at a flow rate of 1.0 mL/

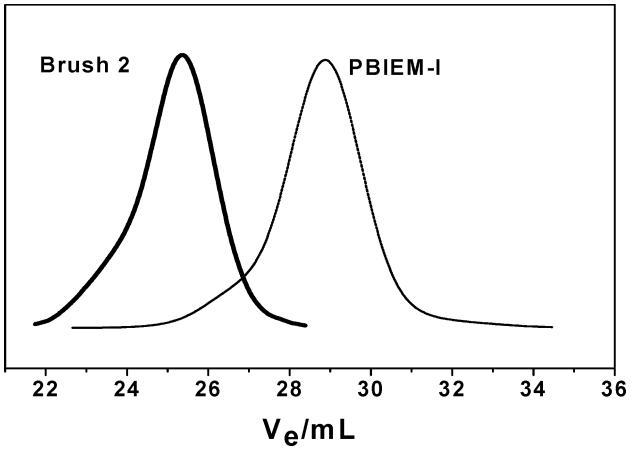

Figure 1. GPC traces of PBIEM-I (DP = 240) and the corresponding short glycocylindrical brush 2 in THF.

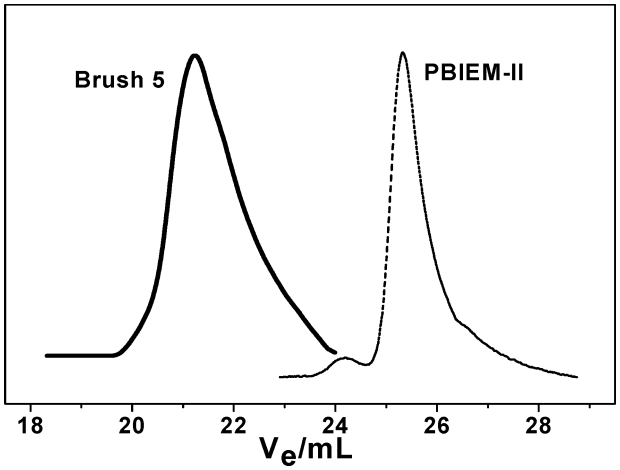

Figure 2. GPC traces of PBIEM-II (DP = 1500) and the corresponding long glycocylindical brush 5 in THF.

min at room temperature. Column set: 5 μm polymer standards service (PSS) SDV gel, 10^2, 10^3, 10^4, and 10^5 Å, 30 cm each. Detectors: Waters 410 differential refractometer and Waters photodiode array detector operated at 254 nm. Narrow PS and poly(methyl methacrylate) (PMMA) standards (PSS, Mainz) were used for the calibration of the column set. GPC with a multiangle light scattering detector (GPC-MALS) and a Viscotek viscosity detector H 502B (GPC/viscosity) were used to determine the absolute molecular weights of the brushes and of the side chains cleaved by solvolysis. THF was used as eluent at a flow rate of 1.0 mL/min. Column set: 5 μm PSS SDV gel, 10^3, 10^5, and 10^6 Å, 30 cm each. Detectors: Shodex RI-71 refractive index detector and Wyatt DAWN DSP-F MALS detector equipped with a 632.8 nm He−Ne laser. The refractive index increment in THF solution of the glycocylindrical brush at 25 °C was determined to be dn/dc = 0.0723 mL/mg using a Chromatix KM-16 laser differential refractometer. The refractive index increment in THF solution of the detached side chains at 25 °C was determined to be dn/dc = 0.065 mL/mg using a PSS DnDc-2010/620 differential refractometer. For GPC/viscosity, the universal calibration principle was used. Linear PMMA standards (PSS, Mainz) were used to construct the universal calibration curve. ^{1}H NMR was recorded with a Bruker AC-250 instrument at room temperature.

Dynamic light scattering (DLS) was performed on an ALV DLS/SLS-SP 5022F compact goniometer system with an ALV 5000/E correlator and a He−Ne laser (λ = 632.8 nm). Prior to the light scattering measurements, the sample solutions were filtered using Millipore Teflon filters with a pore size of 0.45 μm. The measured intensity correlation functions were subjected to CONTIN analysis. Apparent hydrodynamic radii of the glycocylindrical brushes were calculated according to the Strokes−Einstein equation.

The samples for scanning force microscopy (SFM) measurements were prepared either by dip-coating from dilute solutions of brushes in tetrahydrofuran or dioxane/water mixtures, with a concentration of 1 mg/L, onto a freshly cleaved mica surface or by spin-casting onto a carbon-coated mica surface. Carbon-coated mica substrates were prepared using the Balzers MED 010 minideposition system to deposit carbon with a thickness of approximately 5 nm by evaporation. The SFM images were taken with a Digital Instruments Dimension 3100 microscope operated in tapping mode (free amplitude of the cantilever ≈30 nm, set point ratio ≈0.98).

For cryogenic transmission electron microscopy (cryo-TEM) studies, a drop of the sample was put on an untreated bare copper transmission electron microscopy (TEM) grid (600 mesh, Science Services, München, Germany), where most of the liquid was removed with blotting paper, leaving a thin film stretched over the grid holes. The specimens were instantly shock frozen by rapid immersion into liquid ethane and cooled to approximately 90 K by liquid nitrogen in a temperature-controlled freezing unit (Zeiss Cryobox, Zeiss NTS GmbH, Oberkochen, Germany). The temperature was monitored and kept constant in the chamber during all of the sample preparation steps. After freezing the specimens, the remaining ethane was removed using blotting paper. The specimen was inserted into a cryo-transfer holder (CT3500, Gatan, München, Germany) and transferred to a Zeiss EM922 EF-TEM instrument. Examinations were carried out at temperatures around 90 K. The transmission electron microscope was operated at an acceleration voltage of 200 kV. Zero-loss filtered images (ΔE = 0 eV) were taken under reduced dose conditions (100−1000 e/nm^2). All images were registered digitally by a bottom mounted CCD camera system (Ultrascan 1000, Gatan) combined and processed with a digital imaging processing system (Gatan Digital Micrograph 3.9 for GMS 1.4).

Results and Discussion

1. Synthesis and Molecular Characterization of Glycocylindrical Brushes. Synthesis of Protected Cylindrical Brushes. We have previously reported the synthesis of the polyinitiator poly(2-(2-bromoisobutyryloxy)ethyl methacrylate) (PBIEM), where the precursor poly(2-hydroxyethyl methacrylate) (PHEMA) was made via ATRP as well as anionic polymerization.[8] Whereas ATRP led to moderately narrow molecular weight distributions of the backbone ($1.16 < M_w/M_n < 1.24$),[6,8] anionic polymerization led to nearly monodisperse main chains ($M_w/M_n = 1.08$) with a high molecular weight.[8] The number-average molecular weights of the two polyinitiators PBIEM-I and PBIEM-II are 6.68×10^4 and 41.8×10^4, respectively, corresponding to number-average degrees of polymerization of DP_n = 240 and 1500, respectively. By using these polyinitiators, glycopolymer cylindrical brushes with different backbone lengths were obtained.

We recently reported that CuBr/HMTETA and $(PPh_3)_2NiBr_2$ are among the best catalyst systems for the homopolymerization of MAIGlc to obtain linear poly(MAIGlc)s with a narrow molecular weight distribution (MWD).[21] In this work, we chose CuBr/HMTETA for the synthesis of glycocylindrical brushes.

Table 1 represents the results of the synthesis of glycocylindrical brushes by using CuBr/HMTETA as the catalyst system, MAIGlc as the monomer, and PBIEM-I and PBIEM-II as the polyinitiators. It should be noted that the polyinitiator PBIEM-II with the higher molecular weight dissolves in the reaction mixture much slower than PBIEM-I. The time of stirring before the addition of ligand should be long enough to ensure the complete dissolution of polyinitiator. Otherwise, a broad

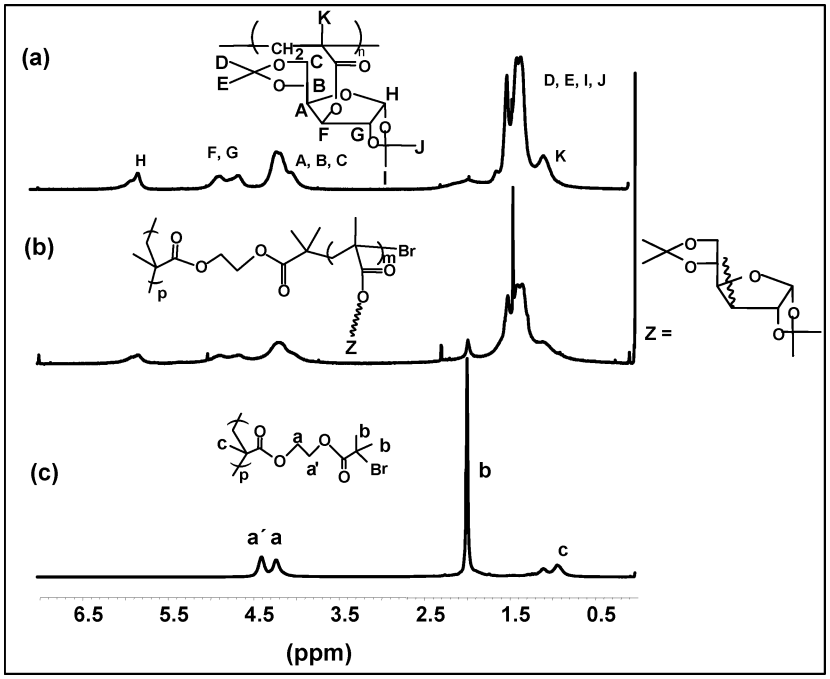

Figure 3. ^{1}H NMR spectra ($CDCl_3$) of (a) linear poly(MAIGlc), (b) cylindrical brush with poly(MAIGlc) side chains (brush 3), and (c) the polyinitiator PBIEM-I.

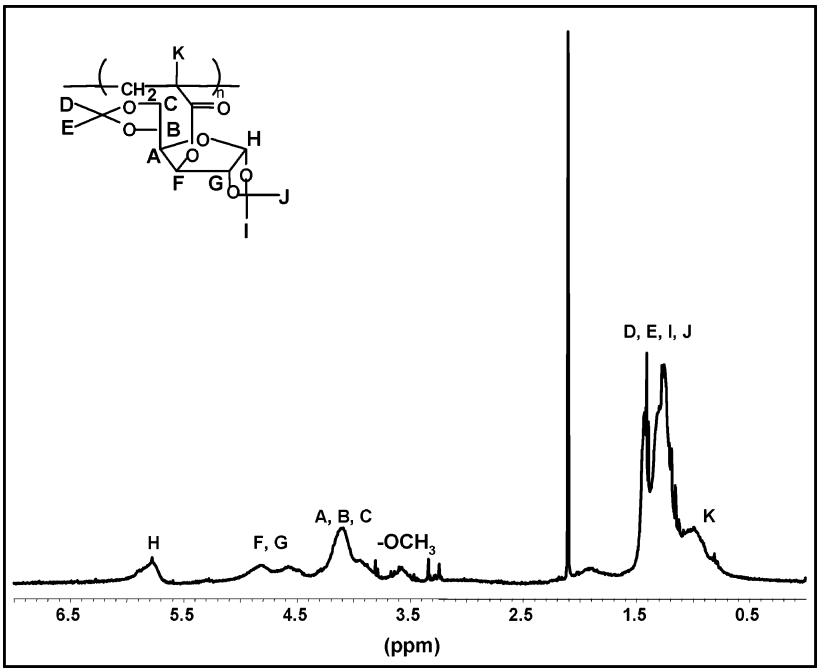

Figure 4. ^{1}H NMR spectrum ($CDCl_3$) of the detached side chains of brush 3.

molecular weight distribution of the final product will result. As can be seen from Table 1, very low conversions are maintained in all cases in order to obtain well-defined glycocylindrical brushes. Even at such low conversions, the reaction mixture becomes very viscous owing to the very high molecular weights of the resulting brushes. The obtained cylindrical brushes with MAIGlc side chains show monomodal GPC eluograms (Figures 1 and 2), and their molecular weight distributions are quite narrow (PDI < 1.25), indicating that intermacromolecular coupling reactions are negligible. Hence, without adding Cu(II) salts,[5] a high ratio of monomer to initiator and a low conversion are sufficient to suppress undesirable side reactions and to obtain the desired glycocylindrical brushes.

The molecular weights of these brushes obtained from GPC using linear PS standards are just the apparent ones. Hence, the true molecular weights of these brushes as well as the radii of gyration (R_g) in THF were determined by GPC-MALS. As can be seen from Table 1, for the same backbone, R_g of the brushes increases with the side chain lengths. The main chain stiffness of the polymer brush increases with increasing side chain length, because the overcrowding of longer side chains forces the otherwise flexible main chain into a more stretched conformation. In addition, at a given DP of side chain (DP_{sc}), a larger R_g was observed for brushes with poly(MAIGlc) side chains compared to brushes with P*t*BA side chains with the same backbone. For instance, in the case of brushes with poly(MAIGlc) side chains,

Table 2. Characterization of Cleaved Side Chains of PMAIGlc Brushes and of Initiation Site Efficiencies (f)[a]

brush	$M_{n,GPC}$[b]	M_w/M_n[b]	$M_{n,GPC/visco}$[c]	M_w/M_n[c]	$M_{n,GPC\text{-}MALS}$[d]	DP_n[e]	f[e] (%)	DP_{bb}/DP_{sc}
3	22 300	1.34	23 900	1.38	23 200	81	27	2.9
4	9000	1.34	13 600	1.40		47	38	32
5	19 100	1.26	27 400	1.35	28 100	96	23	15.6

[a] $f = DP_{n,calcd}/DP_{n,exptl}$. [b] Determined by GPC using THF as eluent with PMMA standards. [c] Determined by GPC/viscosity measurement. [d] Determined by GPC-MALS measurement. [e] Average of GPC/viscosity and GPC-MALS measurements.

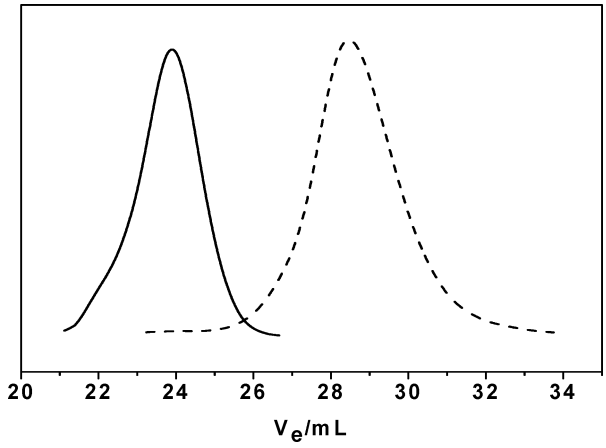

Figure 5. GPC traces of brush 3 (—) and cleaved side chains (– –) after solvolysis.

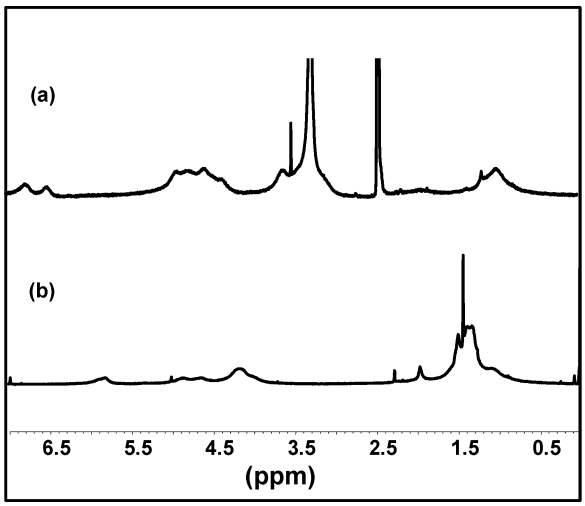

Figure 6. ^1H NMR spectra of deprotected brush 3 with MAGlc side chains (a, d_6-DMSO) and glycocylindrical brush with MAIGlc side chains (b, $CDCl_3$).

R_g = 31.2 nm was obtained at DP_{sc} = 22 for brush 3, whereas R_g = 11.6 nm at DP_{sc} = 28 was observed for P*t*BA synthesized from the same polyinitiator.[8] This could be attributed to the bulky sugar moiety of the monomer (MAIGlc) under study, leading to a stronger stretching of the backbone. The molar masses obtained by light scattering are significantly higher than those obtained by GPC. This is due to the compact nature of the brushes.

Figure 3 represents the ^1H NMR spectra of linear poly(MAIGlc), the polyinitiator, and the glycocylindrical brushes. In Figure 3c, there are two typical peaks at 4.21 and 4.37 ppm (a and a′), which represent the methylene protons between two ester groups of the polyinitiator. After the formation of the brush with poly(MAIGlc) side chains, the characteristic peaks at 1.2–1.4 (isopropylidene protons), 3.8–5.0, and 5.7–6.0 ppm are clearly seen in Figure 3b. This indicates the successful formation of glycocylindrical brushes with poly(MAIGlc) side chains.

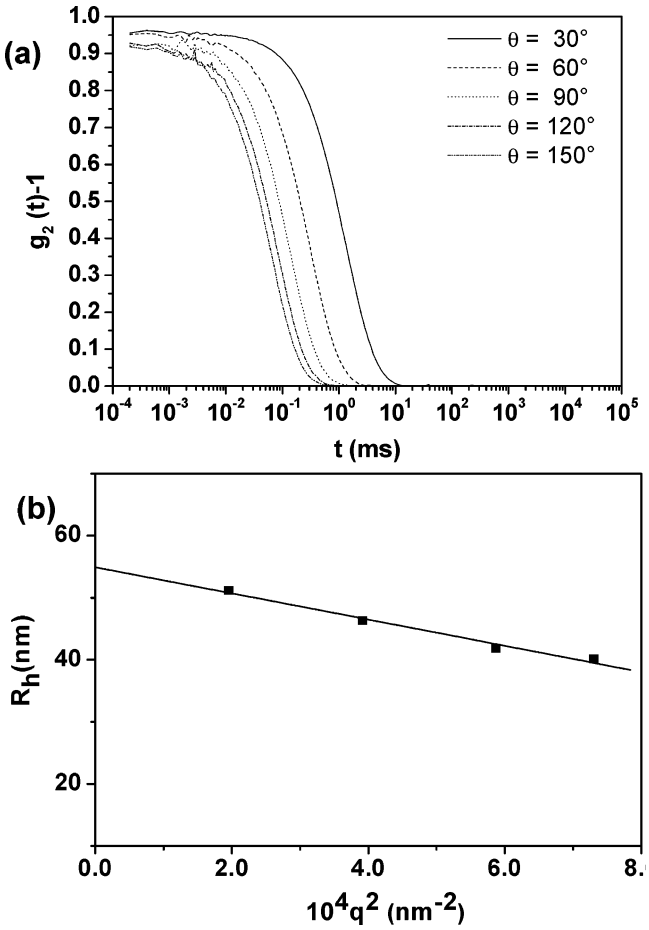

Figure 7. (a) Normalized intensity correlation functions at different scattering angles and (b) dependence of R_h on the square scattering vector for glycocylindrical brush 4 in THF.

Solvolysis of the Glycocylindrical Brushes. To determine the exact side chain length, and thus the initiation site efficiency, the side chains were cleaved from the backbone via base-catalyzed transesterification in methanol. ^1H NMR spectra of the resulting products (cf. Figure 4) revealed that solvolysis with sodium methoxide resulted in side chains consisting of a statistical copolymer of 17% MMA and 83% MAIGlc units. The comonomer composition was determined by comparing the peaks at 3.59 ppm attributed to the methyl ester protons ($-OCH_3$) of the MMA units and the peaks at 5.8–6.0 ppm attributed to the single ring proton of MAIGlc units. Similar results were obtained for brush 4 and brush 5. To calculate the DP of the side chains, the molecular weights of the side chains (see below) were divided by an average molecular weight of the comonomers, M_0 = 290 g/mol.

Table 2 summarizes the detailed characterization of the side chains cleaved by solvolysis and the corresponding initiation efficiencies (f). The GPC traces of

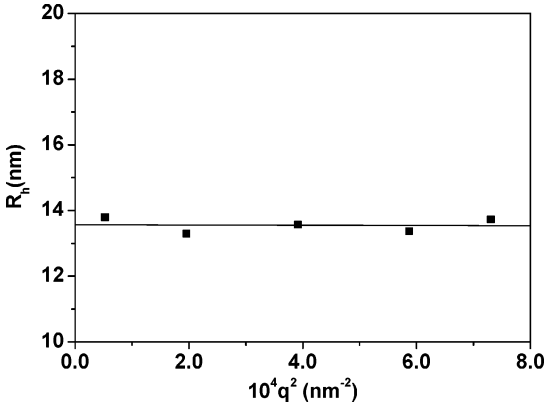

Figure 8. Angular dependence of R_h for short glycocylindrical brush 2 in THF.

brush 3 and the cleaved side chains are given in Figure 5. The monomodal character of the detached side chains shows the absence of the inter- and intramolecular coupling reactions. The absolute molecular weights of the cleaved side chains were determined by using GPC/viscosity and GPC-MALS measurements which allow accurate evaluation of the initiation efficiencies. The polydispersity index of the cleaved arms is $M_w/M_n \cong 1.3$, as can be seen from Table 2, which is a typical value for polymer obtained by slow initiation (limiting $M_w/M_n = 1.33$ for $k_p \gg k_i$ in the Gold distribution[23]). Under these conditions, all monomer is consumed before complete initiation. The initiating efficiency of brush 3 was found to be only 27%, as shown in Table 2. The initiating efficiencies of the PMAIGlc brushes investigated are in the range 23−38%. This value is much smaller that that obtained for the polymerization of styrene using the same polyinitiator, PBIEM.[6] Recently, Matyjaszewski et al.[22] have demonstrated that the initiating efficiency is limited to approximately 50% for the polymerization of MMA using PBIEM. In our study, the increased bulkiness of the monomer, MAIGlc, could contribute to the low initiation efficiency of the brushes. Despite the low grafting efficiency, the bulky sugar moiety of the monomer (MAIGlc) leads to the stronger stretching of the backbone resulting in extended wormlike conformations, as will be discussed below.

Deprotection of the Cylindrical Brushes. The hydrolysis of the isopropylidene groups of the glycocylindrical brushes was performed by treating the samples with formic acid at room temperature.[21,24] The final product was obtained by dialysis against water and freeze-drying. The ^{1}H NMR spectrum of the glycocylindrical brush with poly(3-*O*-methacryloyl-α,*β*-D-glucopyranoside) side chains, abbreviated as poly(MAGlc), is shown in Figure 6a. The signals of the isopropylidene protons (1.2−1.4 ppm) completely disappear after the deprotection, and a broad signal attributed to anomeric hydroxyl groups of the sugar moieties (6.4−7.0 ppm) appears. This shows the quantitative deprotection of the isopropylidene protecting groups. The deprotected short glycocylindrical brushes are white powders, completely soluble in water and methanol but insoluble in THF, chloroform, and acetone (similar to linear poly(MAGlc)). However, the long brushes are only partially soluble in methanol but completely soluble in water and water/dioxane (1/1) mixtures.

2. Solution Properties of the Cylindrical Brushes. Protected Cylindrical Brushes. Dynamic light scattering (DLS) was also used to characterize the glycocylindrical brushes in THF solution. Figure 7a shows the normalized intensity correlation functions of glycocylindrical brush 4 at different scattering angles. The normalized intensity functions were subjected to CONTIN analysis. The angular dependence of R_h for brush 4 is shown in Figure 7b. A very strong angular dependence is observed, indicating the wormlike nature of the glycocylindrical brushes with a very high aspect ratio (ratio between the backbone and the side chain lengths).[25] In contrast to brush 4, the angular dependence for short brush 2 (Figure 8) is much weaker owing to its low aspect ratio. To obtain polymers exhibiting a cylindrical shape, a high aspect ratio is necessary.

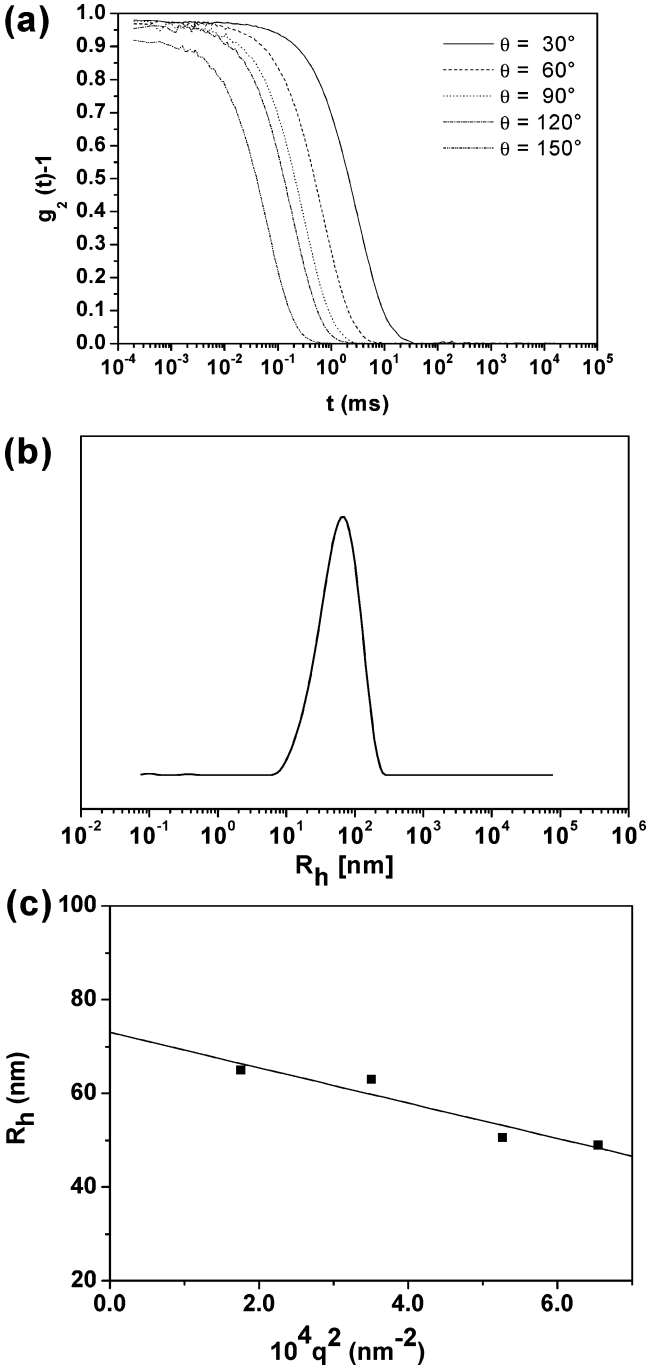

Figure 9. (a) Normalized intensity correlation functions at different scattering angles, (b) the corresponding hydrodynamic radius distribution at a scattering angle of 90°, and (c) dependence of R_h on the square scattering vector for deprotected glycocylindrical brush 4 in water.

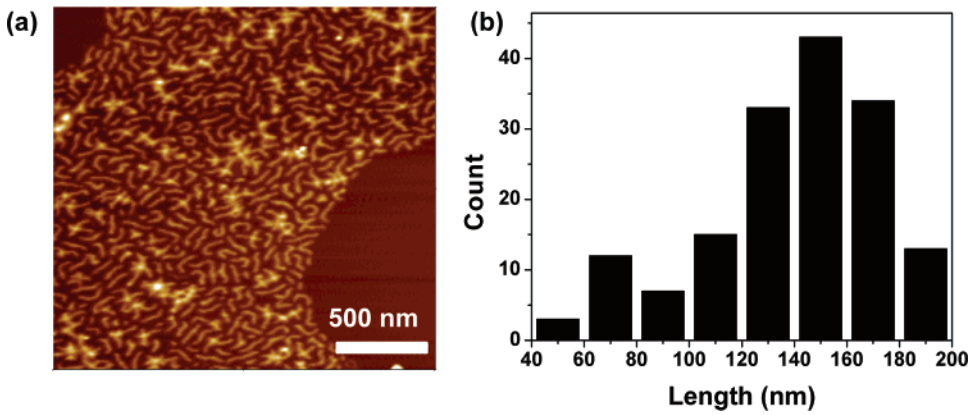

Figure 10. (a) SFM tapping mode height image of brush 5, dip-coated from dilute THF solution on mica (z-range 15 nm) and (b) histogram of the contour length for 160 molecules.

Deprotected Cylindrical Brushes. DLS was performed for deprotected brush 4 in water with a concentration of 0.4 g/L at room temperature (Figure 9). The CONTIN analysis of the autocorrelation functions shows a monomodal hydrodynamic radius distribution at all scattering angles. The hydrodynamic radius distribution of this brush at a scattering angle of 90° in water is shown in Figure 9b. The z-average hydrodynamic radius of this brush at 90° is 63.3 nm. The angular dependence plot of this brush is shown in Figure 9c. Again, the angular dependence of R_h is very strong, indicating its stretched wormlike nature. After extrapolation of q^2 to zero, the hydrodynamic radius of this brush in water is 72.9 nm which is significantly higher than the extrapolated hydrodynamic radius, $R_h = 54.9$ nm, for the same brush in THF before hydrolysis. This indicates that, after hydrolysis, the brushes in water are more stretched owing to the hydration of the sugar moieties. These results are further supported by SFM and cryo-TEM measurements.

3. Visualization of the Cylindrical Brushes by SFM and cryo-TEM. Scanning Force Microscopy of the Protected Cylindrical Brushes. The glycocylindrical brushes were then further characterized by scanning force microscopy (SFM). The protected samples were prepared either by dip-coating from dilute THF solutions using freshly cleaved mica as a substrate or by spin-coating from dilute solutions onto carbon-coated mica.

Figure 10a displays an image of long glycocylindrical brush 5 dip-coated from THF on mica. When the polyinitiator synthesized via anionic polymerization (PBIEM-II) was used, long cylindrical brushes with a narrow backbone length distribution were obtained. The high uniformity as well as the regular cylindrical shape enables us to perform a statistical analysis. The number-average and weight-average lengths of 160 cylinders are $L_n = 138$ nm and $L_w = 147$ nm, respectively, with a polydispersity of $L_w/L_n = 1.06$ which agrees well with the polydispersity of the backbone ($M_w/M_n = 1.08$). The number-average brush length of 138 nm corresponds to the length per main chain monomer unit of 0.09 nm, which is much smaller than the maximum value of 0.25 nm, indicating that the main chain is not completely stretched out but locally coiled. This could be due to the low grafting efficency ($f = 23\%$) of the brush, as discussed earlier.

Figure 11a represents the SFM image of long brush 4, spin-coated from THF onto carbon-coated mica. Carbon-coated mica was chosen in order to avoid problems associated with aggregation and dewetting. Single wormlike macromolecules can be visualized directly. The number-average and weight-average lengths of 20 individual cylinders in Figure 11a are $L_n = 110$ nm and $L_w = 114$ nm, respectively, with a polydispersity of $L_w/L_n = 1.04$. These brushes are somewhat shorter than brush 5, possibly due to the shorter side chains (DP = 47 vs 96), although their grafting density is higher than that of brush 5 ($f = 38$ vs 23%).

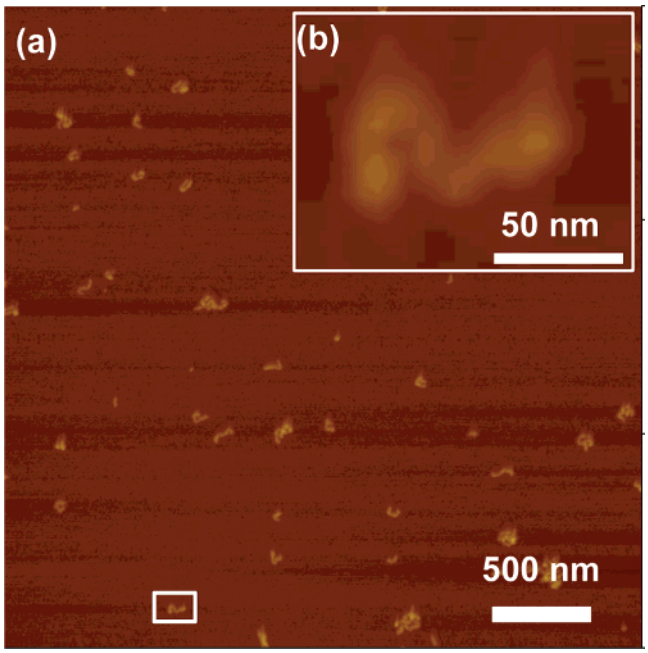

Figure 11. (a) SFM tapping mode height image of brush 4, spin-coated from dilute solution on carbon-coated mica (z-range 20 nm) and (b) 5× magnification of the single cylinder marked by a rectangle in part a.

SFM of the Deprotected Brushes. Figure 12 shows a SFM image of deprotected long brush 4, spin-coated from a dioxane/water mixture (volume ratio of 1/1) onto mica. Wormlike macromolecules could be visualized, indicating that the structure is preserved during deprotection. The number- and weight-average lengths of 40 cylinders are $L_n = 130$ nm and $L_w = 134$ nm, respectively, with a polydispersity of $L_w/L_n = 1.03$. The cylinders appear to be more stretched than those before hydrolysis ($L_n = 110$ nm). The cylinders are still much shorter than the maximum contour length of cylinders in the fully stretched state. These results are quite compatible with the results obtained from DLS mea-

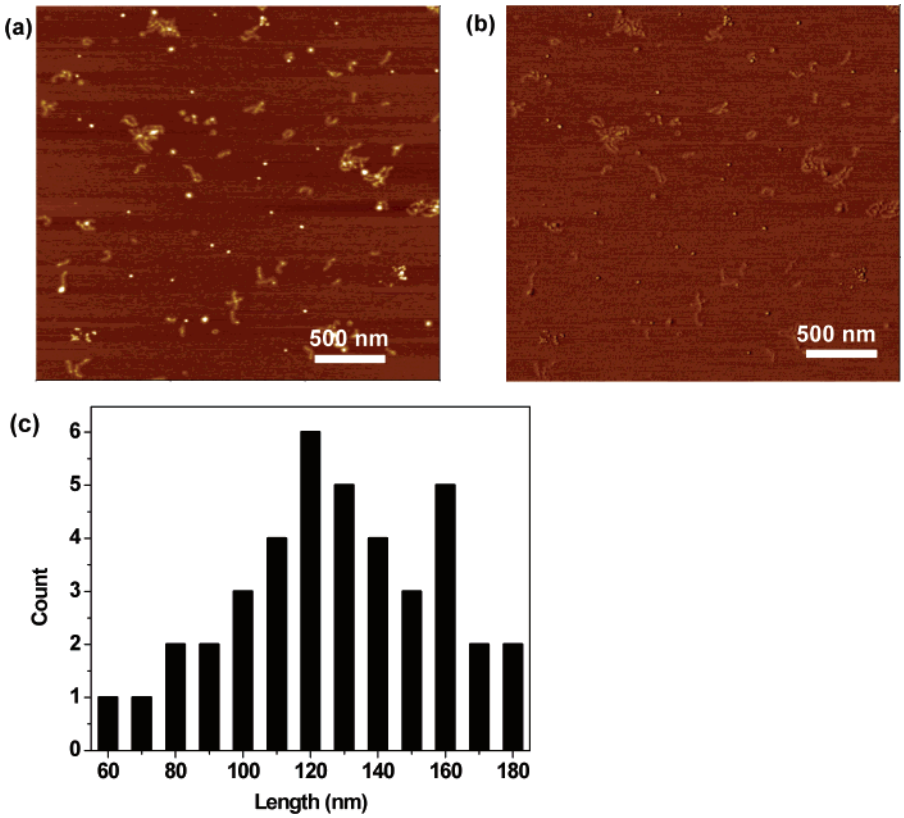

Figure 12. SFM tapping mode images of deprotected brush 4, spin-coated from dilute water/dioxane (1/1) solution on mica: (a) height image (z-range 10 nm); (b) phase image (range 40°). (c) Histogram of the contour length for 40 molecules.

surements for brush 4 in water ($R_h(q^2 \rightarrow 0) = 72.9$ nm). The curvature of the brushes is higher than expected. To check whether this is due to the interaction of the molecule with the substrate, cryo-TEM measurements in water were performed, as discussed in the next section.

Cryogenic Transmission Electron Microscopy (cryo-TEM) Characterization of Deprotected Glycocylindrical Brushes. The structure of deprotected glycocylindrical brush 4 in aqueous solution was characterized using cryo-TEM. This tool allows one to directly image the original shape and size of the polymers in solution, since the sample is vitrified before the measurement. The cryo-TEM image of deprotected brush 4 (Figure 13) shows wormlike cylinders. The magnification of a single cylinder is also shown as an inset, and the length of that single cylinder is found to be 130 nm which agrees very well with the length of deprotected brush 4 obtained by SFM measured in the dry state.

Conclusions

We have demonstrated that the CuBr/HMTETA catalyst system could be successfully employed for the homopolymerization of MAIGlc in the grafting from process, leading to well-defined glycocylindrical brushes or "sugar sticks". The deprotection of the isopropylidene protecting groups resulted in water-soluble glycocylindrical brushes. The extensive characterization of the water-soluble brushes by DLS, SFM, and cryo-TEM confirms their stretched, wormlike structure. Analysis of the side chains detached by basic solvolysis indicated that the grafting efficiency was approximately $0.20 < f < 0.40$. Thus, although the side chains are not as densely spaced as those for some PS or polyacrylate brushes, their behavior is typical rather for cylindrical brushes than comb-shaped polymers. Such brushes with carbohydrate moieties in the side chains can be manipulated for various biological and medicinal applications. Such investigations are in progress.

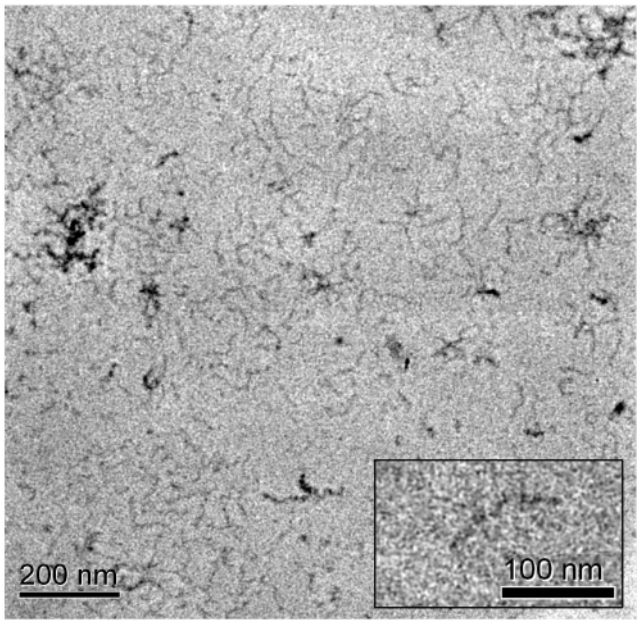

Figure 13. cryo-TEM image of deprotected long brush 4.

Acknowledgment. This work was supported by the Deutsche Forschungsgemeinschaft (Grant No. Mu 896/14). We wish to thank Prof. Werner Köhler for his useful suggestions regarding DLS measurements. Clarrisa Abetz is acknowledged for the preparation of the carbon-

coated mica substrate. We also very much appreciate the constructive comments of the reviewers.

References and Notes

(1) Tsukahara, Y.; Mizuno, K.; Segawa, A.; Yamashita, Y. *Macromolecules* **1989**, *22*, 1546−1552.
(2) Djalali, R.; Hugenberg, N.; Fischer, K.; Schmidt, M. *Macromol. Rapid Commun.* **1999**, *20*, 444−449.
(3) Schappacher, M.; Billaud, C.; Paulo, C.; Deffieux, A. *Macromol. Chem. Phys.* **1999**, *200*, 2377−2386.
(4) Ryu, S. W.; Hirao, A. *Macromolecules* **2000**, *33*, 4765−4771.
(5) Beers, K. L.; Gaynor, S. G.; Matyjaszewski, K.; Sheiko, S. S.; Möller, M. *Macromolecules* **1998**, *31*, 9413−9415.
(6) Cheng, G.; Böker, A.; Zhang, M.; Krausch, G.; Müller, A. H. E. *Macromolecules* **2001**, *34*, 6883−6888.
(7) Li, C.; Gunari, N.; Fischer, K.; Janshoff, A.; Schmidt, M. *Angew. Chem., Int. Ed.* **2004**, *43*, 1101−1104.
(8) Zhang, M.; Breiner, T.; Mori, H.; Müller, A. H. E. *Polymer* **2003**, *44*, 1449−1458.
(9) Zhang, M.; Drechsler, M.; Müller, A. H. E. *Chem. Mater.* **2004**, *16*, 537−543.
(10) Zhang, M.; Teissier, P.; Krekhova, M.; Cabuil, V.; Müller, A. H. E. *Prog. Colloid Polym. Sci.* **2004**, *126*, 35−39.
(11) Zhang, M.; Estournes, C.; Bietsch, W.; Müller, A. H. E. *Adv. Funct. Mater.* **2004**, *14*, 871−882.
(12) Lee, Y. C.; Lee, R. T. *Acc. Chem. Res.* **1995**, *28*, 321−327.
(13) Wassarman, P. M. *Science* **1987**, *235*, 553−560.
(14) Chen, X. M.; Dordick, J. S.; Rethwisch, D. G. *Macromolecules* **1995**, *28*, 6014−6019.
(15) Dordick, J. S.; Linhardt, R. J.; Rethwisch, D. G. *CHEMTECH* **1994**, *24*, 33−39.
(16) Klein, J.; Kunz, M.; Kowalczyk, J. *Makromol. Chem., Macromol. Chem. Phys.* **1990**, *191*, 517−528.
(17) Li, Z. C.; Liang, Y. Z.; Chen, G. Q.; Li, F. M. *Macromol. Rapid Commun.* **2000**, *21*, 375−380.
(18) Liang, Y. Z.; Li, Z. C.; Chen, G. Q.; Li, F. M. *Polym. Int.* **1999**, *48*, 739−742.
(19) Ejaz, M.; Ohno, K.; Tsujii, Y.; Fukuda, T. *Macromolecules* **2000**, *33*, 2870−2874.
(20) Muthukrishnan, S.; Jutz, G.; André, X.; Mori, H.; Müller, A. H. E. *Macromolecules* **2005**, *38*, 9−18.
(21) Muthukrishnan, S.; Mori, H.; Müller, A. H. E. *Macromolecules* **2005**, *38*, 3108−3119.
(22) Neugebauer, D.; Sumerlin, B. S.; Matyjaszewski, K.; Goodhart, B.; Sheiko, S. S. *Polymer* **2004**, *45*, 8173−8179.
(23) Gold, L. *J. Chem. Phys.* **1958**, *28*, 91.
(24) Ohno, K.; Tsujii, Y.; Fukuda, T. *J. Polym. Sci., Part A: Polym. Chem.* **1998**, *36*, 2473−2481.
(25) Dentini, M.; Coviello, T.; Burchard, W.; Crescenzi, V. *Macromolecules* **1988**, *21*, 3312−3320.

MA0515073